

Article

Geochemical Assessment and Mobility of Undesired Elements in the Sludge of the Phosphate Industry of Gafsa-Metlaoui Basin, (Southern Tunisia)

Olfa Smida ^{1,2,*} , Radhia Souissi ², Marzougui Salem ^{1,2} and Fouad Souissi ^{1,2}

¹ University of Tunis El Manar, Faculty of Sciences of Tunis, Department of Geology, Tunis 2092, Tunisia; mar_706@outlook.com (M.S.); souissifoued2@gmail.com (F.S.)

² Institut National de Recherche et d'Analyse Physico-Chimique (INRAP), Laboratoire des Matériaux Utiles, Technopark of Sidi Thabet, Ariana 2020, Tunisia; souissiradhia@yahoo.fr

* Correspondence: smidaolfa@gmail.com; Tel.: +216-96-518-566

Abstract: The raw phosphates in the Gafsa-Metlaoui phosphate basin are valorized by wet processes that are performed in the laundries of the Gafsa Phosphates Company (CPG, Gafsa, Tunisia) to reach market grades (>28% P₂O₅). This enrichment process allows the increase of P₂O₅ content by the elimination of the coarse (>2 mm) and fine (<71 μm) fractions. Mineralogical analysis has shown that all the investigated materials (raw phosphate, marketable phosphate, coarse waste, and fine waste) from the laundries of M'Dhilla-Zone L and Redeyef are both composed of carbonate fluorapatite, carbonates, quartz, gypsum, clays, and clinoptilolite. Chemical analysis shows that Cr, Cd, Zn, Pb, and U are concentrated in the fine wastes and associated with the clay-phosphate fraction. The rare earth elements are more concentrated in both raw and marketable phosphates. Drilling and sludge-water analysis, along with leaching tests conducted on the fine wastes, showed that, due to phosphate industry, cadmium, fluorine, and sulfate contributing to the pollution of water resources in the region, pollution is more conspicuous at M'Dhilla.

Keywords: phosphate industry; sludge; metals; mobility; batch tests



Citation: Smida, O.; Souissi, R.; Salem, M.; Souissi, F. Geochemical Assessment and Mobility of Undesired Elements in the Sludge of the Phosphate Industry of Gafsa-Metlaoui Basin, (Southern Tunisia). *Appl. Sci.* **2021**, *11*, 1075. <https://doi.org/10.3390/app11031075>

Academic Editor: Juan García Rodríguez
Received: 26 December 2020
Accepted: 19 January 2021
Published: 25 January 2021

Publisher's Note: MDPI stays neutral with regard to jurisdictional claims in published maps and institutional affiliations.



Copyright: © 2021 by the authors. Licensee MDPI, Basel, Switzerland. This article is an open access article distributed under the terms and conditions of the Creative Commons Attribution (CC BY) license (<https://creativecommons.org/licenses/by/4.0/>).

1. Introduction

The Gafsa-Metlaoui phosphate basin that is managed by the Compagnie des Phosphates de Gafsa (CPG, Gafsa, Tunisia) is the most important mining area in Tunisia. It includes large-scale phosphate-extraction industry activities, with an annual production rate of around 3.34 million tons in 2018 [1]. Most of the phosphate ores are not suitable for immediate use in the processing industry, due to their relatively low P₂O₅ content and generally their content of a series of gangue minerals. Thus, they shall undergo prior enrichment before being employed in the acidulation process [2]. Upgrading processes of sedimentary-type phosphate ores to reach marketable grades (P₂O₅ > 28%) consist of separating the gangue minerals (silicates and carbonates) from the valuable phosphate material [3]. The CPG in the Gafsa-Metlaoui Basin is equipped with ten laundries, in which phosphates are enriched by wet processing according to the following steps: phosphate ore is extracted from quarries, then transported by trucks and conveyors to laundries, then scalped to 120 mm. At a later stage, the fraction >120 mm is considered sterile and evacuated to the rock dumps, while the fraction <120 mm is crushed and screened at 40 mm to feed the scrubbers. In the present work, the ore with a grain size <40 mm, resulting from these last operations (scalping, crushing, and screening), is considered as raw phosphate (RP).

The scrubbing consists of shaking the raw ore with water for 2 min to 3 min, followed by washing on a 2 mm mesh-vibrating screen. This first operation of particle-size grading consists of paring the high cut; the particles >2 mm in diameter make the coarse waste (CW) at the factory. The fraction <2 mm is meant for the supply of hydrocyclones, in order

to eliminate fine wastes (FW) in the form of mud with a particle size $<71 \mu\text{m}$. The final product matches the marketable phosphates (MP) with a particle size ranging from 2 mm to $71 \mu\text{m}$ [4].

The water that is required to wash the phosphate ore is provided by deep boreholes often located nearby the laundries. Due to the excessive consumption of drilling water (DW), the CPG has opted, for many years now, for another strategy that consists of recycling water from the washing circuit. This process is conducted by recovering water from the settling pond and mixing it with new drilling water. In this work, the discharge filtrates are sludge water (SW), which is recovered from the natural decantation of the sludge collected from the laundries.

At the laundries, the process water is recycled after recovery from the sludge by flocculation in settling ponds. Once settled, the resulting thick mud is discharged either to tailings disposal impoundments or into the hydrographic network. However, these fine wastes (FW) may contain mineral fractions carrying undesired elements such as Cd, U, Zn, F^- , NO_3^- , PO_4^{3-} , etc. Several scholars have focused on both mineralogical and geochemical studies of solid discharges from laundries [5–8], but without establishing a geochemical assessment between the input and output products of the phosphate laundries.

Other scholars have focused on the impact generated by heavy metals from these discharges at the soil–plant interface [7–10], but they did not highlight the influence of mineralogy and geochemistry of the solid effluents on the mobility of metallic trace elements (MTE).

In this study, we have tried, firstly, to determine the mineralogical and geochemical characterization of the input and output products of the two laundries of Zone L (ZL) of M'Dhilla and Redeyef, which are installed east and west of the Gafsa-Metlaoui Basin, respectively. Second, this work is innovative in terms of mobility assessment of MTE (Cd and U) contained in the sludge being discharged by the aforementioned laundries, with reference to batch tests.

2. Materials and Methods

2.1. Study Area

Covering an area of approximately 5.000 km^2 to 6.000 km^2 , the Gafsa phosphate basin (Figure 1) is located in the southern Tunisian Atlas region. It is bounded, to the north, by the Gafsa fault, to the east by the north Chotts chain, to the west by the Algerian territory, and to the south by the Saharan platform.

Weather data (temperature, rainfall, wind, humidity, and evaporation) prevailing in the region are coterminous with pre-desert climatic characteristics, whereas the M'Dhilla and Redeyef zones are characterized by a cool lower -arid bioclimatic belt.

Only the exploitable phosphate ore from the Metlaoui formation of Upper Paleocene–Lower Eocene age, which contains the main phosphate series of the mining basin, will be taken into consideration in this study.

2.2. Phosphates Deposits

Sedimentary phosphate deposits result from the long-term active sedimentation in the sea and account for more than 80% of phosphate ore production in the world.

Natural phosphates include more than 200 mineralogical species. The most abundant belong to the apatite group, which make a family of solid isomorphous fluorapatite compounds with the formula $\text{Ca}_{10}(\text{PO}_4)_6\text{F}_2$.

Fluorapatite is the most common phosphate mineral in igneous rocks. In this mineral, fluorine can be partially replaced by OH or Cl.

In the phosphate minerals of sedimentary deposits, the corresponding phosphate minerals are related to fluorapatite. They differ from this mineral by a set of partial isomorphous substitutions. The most marked substitution in sedimentary apatites is that of PO_4^{3-} by CO_3^{2-} , accompanied by the introduction of additional F^- ions to preserve

electrical neutrality. The mineral obtained is carbonate fluorapatite (CFA) with a simplified structural formula $\text{Ca}_{10}((\text{PO}_4)_{6-x}(\text{CO}_3\text{F})_x)\text{F}_2$.

Other substitutions may also occur, consisting essentially in the partial replacement of Ca by Na, Mg, or Sr; of F by OH; and of PO_4 by SO_4 , VO_4 , SiO_4 , AsO_4 , etc.

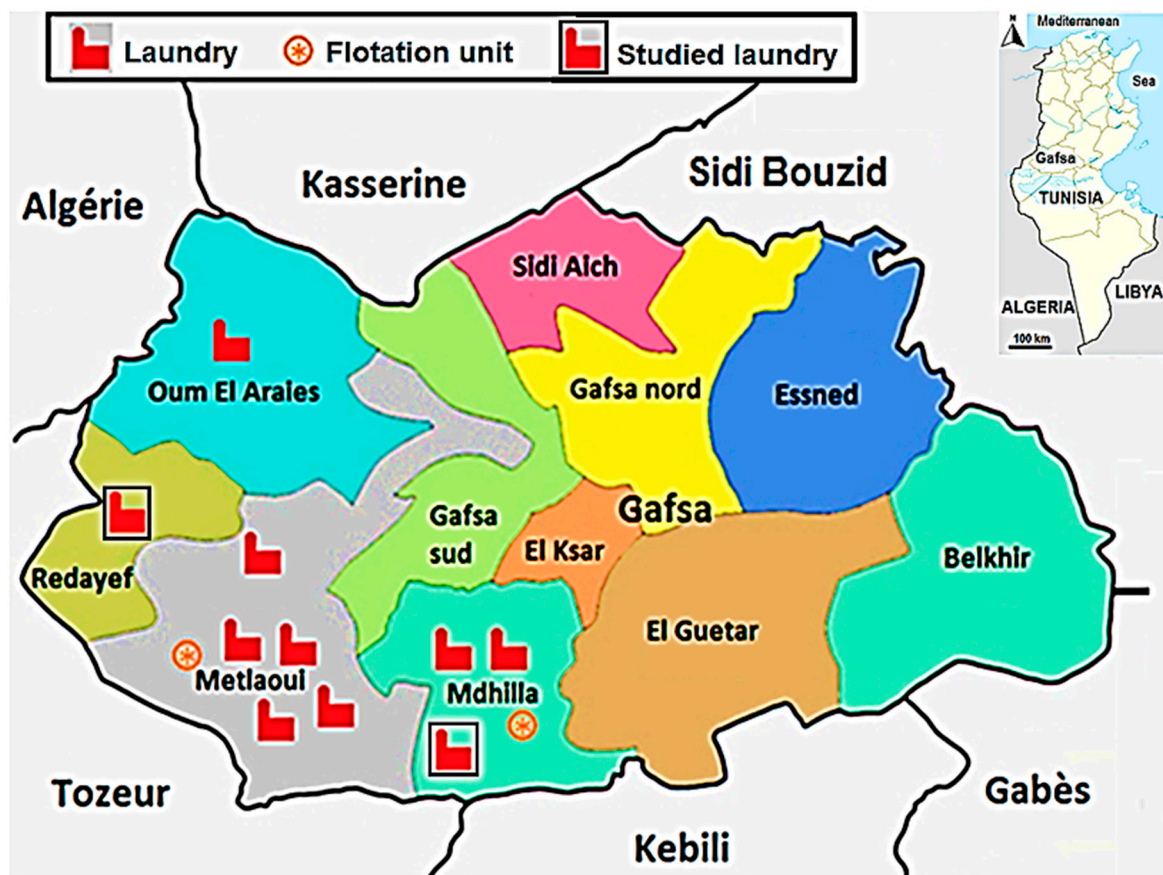


Figure 1. Location map of phosphate laundries in the Gafsa-Metlaoui Basin.

2.3. Sampling and Preparation

A series of samples of the input and output products were taken in the laundries. The samples selected from the same washing circuit are raw phosphate (RP), marketable phosphate (MP), coarse waste (CW), fine waste (FW), drilling water (DW), recycled water (RW), and sludge water (SW). The sampling procedure was the same for both laundries (Redeyef and M'Dhilla-Zone L). A total of 14 samples were collected from the two laundries—six water samples (DW, RW, and SW) and eight solid samples (RP, MP, CW, and FW). About two kilograms of each solid sample were collected and kept in plastic bags. Sludge samples were decanted naturally for 24 h in order to separate water from the solid residue.

In the laboratory, all the water samples were filtered to $0.45 \mu\text{m}$ with a cellulose acetate filter. The filtered water was acidified to pH 2.0 with nitric acid to be analyzed by inductively coupled plasma-atomic emission spectroscopy (ICP-AES). The solid samples (RP, MP, CW, and FW) were dried at 60°C for 24 h. Because the size distribution of the sludge was determined by the wet method, the rest of the samples were sieved to 2 mm to be used for the characterization of the main physicochemical properties of input and output products—(i) particle size determination, (ii) mineralogical analysis, (iii) geochemical analysis, and (iv) leaching tests.

2.4. Methods

The collected samples were submitted to particle size, mineralogical, and chemical analyses. The grain-size distribution was performed using a laser analyzer (Malvern Mas-

tersizer 2000, Malvern Panalytical, Malvern, UK). The total calcium carbonate content (%CaCO₃) was carried out by means of a Bernard calcimeter (Gabbrielli Technology, Calenzano, Italy). The organic carbon (C_{org}) and nitrogen (N) rates were successively determined by an elementary micro analyzer carbon/sulfur (Horiba-Jobin, Yvon, Edison, NJ, USA), and the nitrogen was assessed by means of a UDK 132 semi-automatic distillation unit, VELD SCIENTIFICA, Usmate velate (MB), Italy. The organic matter (OM) content was determined by multiplying C_{org} by 1.72 (Van Bemmelen factor, [11]). The mineralogical analyzes were carried out by a PANalyticalX'Pert Pro X-ray diffractometer (XRD, PANalytical, Almelo, The Netherland).

The chemical analysis of the major elements (Ca, Al, Mg, Fe, Si, K, P, and Na) was carried out by fluorescent spectroscopy (XRF, PANalyticalMagix PW2403, PANalytical, Almelo, The Netherland) on pearls obtained by fusion. The detection limits (DL) for the analyzed elements were 0.6 mg/kg, 0.04 mg/kg, 0.01 mg/kg, 0.08 mg/kg, 0.16 mg/kg, 0.01 mg/kg, 0.4 mg/kg, and 0.01 mg/kg, respectively.

For trace (Cd, Cr, Pb, Zn, U, and Sr) and rare earth (La, Ce, Sm, Nd, Eu, Gd, Tb, and Yb) elements analysis, samples were sieved to −2 mm, then finely grounded in an agate mortar and dissolved in a triacid solution (HClO₄, HF, and HNO₃). The measurements were carried out by inductively coupled plasma-atomic emission spectroscopy (ICP–AES, Activa of Horiba-Jobin Yvon, Horiba scientific, Edison, NJ, USA). For the trace elements, the DLs were 0.2 mg/kg, 3.4 mg/kg, 0.53 mg/kg, 1.6 mg/kg, 1 mg/kg, and 8 mg/kg, respectively, and for the rare earth elements, the DLs were 2 mg/kg, 4 mg/kg, 0.8 mg/kg, 8 mg/kg, 0.2 mg/kg, 0.2 mg/kg, 0.2 mg/kg, and 0.1 mg/kg, respectively. The distribution of rare-earth elements (REEs) is displayed as a semi-logarithmic graphical representation where concentrations are normalized to the upper continental crust (UCC) [12].

For the analysis of water samples, the concentrations of anions (NO₂[−], NO₃[−], F[−], PO₄^{3−}, and SO₄^{2−}) were determined by ion chromatography (Shimadzu, Kyoto, Japan). The DLs were 0.01 mg/L; 0.1 mg/L, 0.1 mg/L, 0.1 mg/L, and 0.1 mg/L, respectively. The contents of trace elements (Cd, Fe, Pb, Zn, and U) were determined by ICP–AES. The DLs were 0.0002 mg/L, 0.0023 mg/L, 0.0005 mg/L, 0.0016 mg/L, and 0.001 mg/L, respectively. The chemical analysis, conducted on the certified reference material (BCR-32), showed that the error margin did not exceed 5%.

In most cases, mobility designates the ability of an element to migrate in space, to shift from one chemical form to another, or to undergo a phase change (mainly from a solid phase to a liquid one) [13]. The transfer processes between the two phases (solid and liquid) are multiple; they strongly depend on the nature of the link between the elements being considered, in addition to the solid phase, which is also known as the carrier or retention phase, and the physico-chemical conditions prevalent in the environment. Several physical and chemical processes at the solid–liquid interface generally allow the trapping of metals, such as (physical and chemical) adsorption [14,15], precipitation [16–18], substitution in the crystal lattice, and mechanical trapping.

Leaching is a method for removing soluble components from a solid matrix [19,20]. The batch extraction procedure is a short-term leaching test intended to estimate the release potential of constituents from waste materials over a range of environmental conditions [21], and to evaluate potential risks to human and/or groundwater [22]. It takes into account the nature and particle size of the solid sample, the nature and the pH of the solution, as well as operating conditions such as the liquid/solid ratio (L/S), temperature, contact time, number of extractions, or even the stirring mode [21–25].

In order to assess the mobility of MTE in the fine wastes from the two laundries, batch extraction tests were performed on dried and sieved (2 mm) solid fractions of the sludges, according to the protocols of Kosson et al. [21] and Garrabrants et al. [25], which were adapted to genuine conditions of this study (particle size < 2 mm, sludge water as extractant, liquid to solid (L/S) ratio of 2/1, natural pH). The procedure consists of mixing 10 g of dried sludge with 20 mL of fresh sludge water in a 50 mL polyethylene tube, and then the suspension was subjected to rotary (20 rpm) agitation (end-over-end) for 48 h.

Thereafter, the suspension was centrifuged at $2500 \times g$ rpm for 20 min. Following the recovery of the supernatant by filtration using $0.45 \mu\text{m}$ cellulosic acetate membrane, the pH and Electrical Conductivity (EC) measurement were taken with a multi-parameter (WTW, Xylem analytics, Beverly, MA, USA), and cadmium and uranium concentrations were determined with an inductive plasma coupled with a mass spectrometer (ICP-MS) (Thermo Scientific X-series 2, Thermo fisher scientific, Waltham, Massachusetts, United States). The DL for these elements was $0.001 \mu\text{g/L}$. The solid residue was mixed again with 20 mL of fresh sludge water to perform a new leaching cycle. The whole batch experience was carried out over seven extraction cycles. All preparations and analyses were performed in the laboratories of the National Institute of Research and Physico-Chemical Analysis (INRAP, Technopole of Sidi Thabet, Ariana, Tunisia).

3. Results and Discussion

3.1. Characterization of the Inputs and Output Products of the Phosphate Laundries

The samples collected from the laundries (RP, MP, CW, and FW), were submitted to a particle-size, mineralogical, and geochemical analyses.

3.1.1. Particle-Size Analysis

The results of particle-size analyses of the different phosphate samples from the two laundries are shown in Table 1, taking into account only the fractions of less than 2 mm. The raw (RP) and marketable (MP) phosphates of the two laundries are dominated by fine to very fine sandy texture with percentages ranging from 65% to 66% and from 69% to 78%, respectively. They are also characterized by average contents of medium to coarse sand-sized, ranging from 23.6% to 24.7% and from 21.7% to 30.6%, respectively. It should be noted that the fine waste that was recovered at the outlet of the hydrocyclones has displayed large percentages (58.87% for M'Dhilla-Zone L and 82.84% for Redeyef) of fine fraction ($<63 \mu\text{m}$). However, due to occasional problems, the particle size of wastes at the outlet of hydrocyclones, which is supposed to be lower than $71 \mu\text{m}$, can go up to $400 \mu\text{m}$.

Table 1. Particle-size distribution (% of dry sample). RP: raw phosphate; MP: marketable phosphate, and FW: fine waste from M'Dhilla-Zone L (ZL) and Redeyef (R) laundries.

Fraction	Sample					
	RP-ZL	MP-ZL	FW-ZL	RP-R	MP-R	FW-R
Medium and coarse sand ($250 \mu\text{m} < X < 2 \text{ mm}$)	24.7	30.62	6.45	23.64	21.76	1.07
Fine to very fine sand ($63 \mu\text{m} < X < 250 \mu\text{m}$)	65	69.42	34.5	66.54	78.23	15.94
Medium to coarse silt ($16 \mu\text{m} < X < 63 \mu\text{m}$)	7.2	0	24.8	7.20	0	35.37
Fine to very fine silt ($2 \mu\text{m} < X < 16 \mu\text{m}$)	2.83	0	32.94	2.51	0	45.87
Clay ($X < 2 \mu\text{m}$)	0	0	1.13	0	0	1.6

3.1.2. Mineralogy

The X-ray diffraction mineralogical study was performed on the solid samples (RP, MP, CW, and FW) from the two laundries. In all samples, the results have confirmed the presence of the following minerals: carbonate-fluorapatite CFA ($\text{Ca}_5(\text{PO}_4, \text{CO}_3)_3\text{F}$), clinoptilolite ($(\text{Na}_2, \text{Ca}, \text{K}_2)(\text{Al}_2\text{SiO}_{22})6 \cdot 7\text{H}_2\text{O}$), calcite (CaCO_3), dolomite ($\text{Ca}, \text{Mg}(\text{CO}_3)_2$), ankerite ($\text{Ca}(\text{Fe}, \text{Mg}, \text{Mn})(\text{CO}_3)_2$), gypsum ($\text{CaSO}_4 \cdot 2\text{H}_2\text{O}$), and quartz (SiO_2), with percentages varying according to the samples being employed (Figure 2). The similarity in the mineralogical composition between the input and the output products indicates that the processes of ore treatment in the washing units do not alter the mineralogy. Other silicates, such as smectite ($(\text{Si}_{3+x}\text{Al}_{1-x})\text{O}_{10}(\text{Al}_{2-y}\text{Mg}_y)(\text{OH})_2\text{M}+\text{I}_{1-(x-y)}(\text{H}_2\text{O})_n$) and palygorskite ($(\text{Mg}, \text{Al})_2\text{Si}_4\text{O}_{10}(\text{OH}) \cdot 4(\text{H}_2\text{O})$), are present in the fine wastes from the two laundries. However, regarding clinoptilolite, it was revealed that this mineral is more abundant in the fine waste of the Redeyef laundry (Table 2).

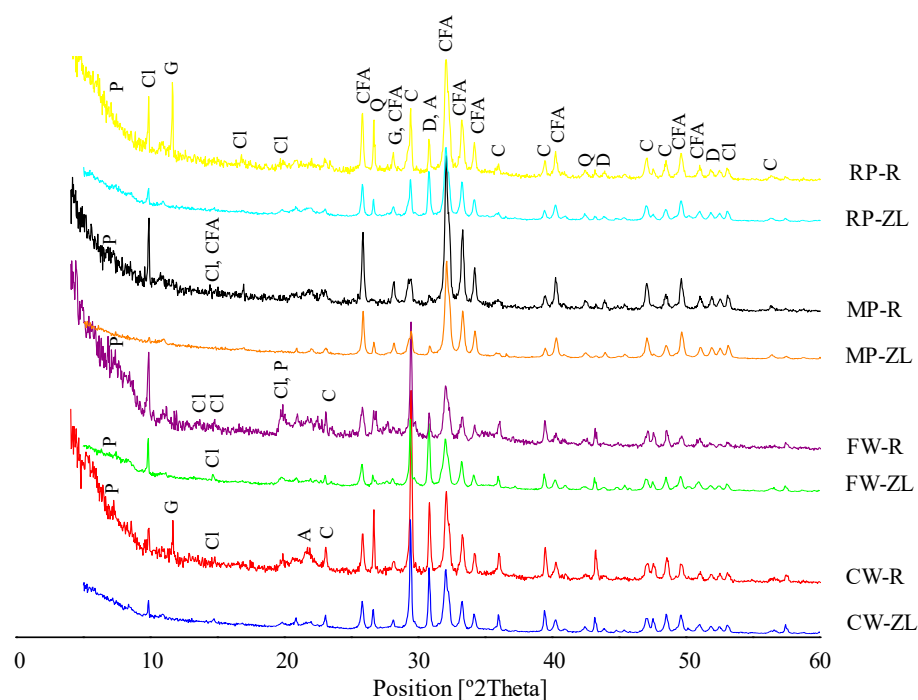


Figure 2. X-rays diffractograms. RP-ZL, MP-ZL, CW-ZL, and FW-ZL: raw phosphate, marketable phosphate, coarse waste, and fine waste from M'Dhilla-Zone L, respectively. RP-R, MP-R, CW-R, and FW-R: raw phosphate, marketable phosphate, coarse waste, and fine waste from Redeyef, respectively. CFA: carbonate fluorapatite, D: dolomite, C: calcite, Q: quartz, A: ankerite, G: gypsum, Cl: clinoptilolite, and P: palygorskite.

Table 2. Semi-quantitative mineralogical composition (%). CW: coarse waste from the M'Dhilla-Zone L (ZL) and Redeyef (R) laundries (other references are as in Table 1).

Mineralogy	Sample							
	RP-ZL	MP-ZL	CW-ZL	FW-ZL	RP-R	MP-R	CW-R	FW-R
Carbonate fluorapatite(CFA)	34	48.5	26.3	23.2	27.3	35.7	16.2	17
Calcite	8	7.9	23.2	16.2	9.1	4.1	22.2	18
Ankerite	13	3	12.1	14.2	6.1	2	6.1	2
Dolomite	14	5	16.2	17.2	6.1	2	9.1	4
Clinoptilolite	23	27.7	18.2	24.2	25.3	37.8	17.2	34
Gypsum	6	6.9	3	3	8.1	5.2	4	4
Quartz	2	1	1	1	5.1	1	9	1
Palygorskite	-	-	-	1	12.9	12.2	16.2	20

3.1.3. Geochemistry

Results of the geochemical analysis of the input and output products from the two laundries are summarized in Table 3.

These results show considerable amounts of OM in the samples in particular those of the Redeyef (1.22–3.89%). This is one of the characteristics of the phosphorites of the Gafsa-Metlaoui Basin. It should be also noted that the raw phosphates and the fine wastes from the two laundries contain the highest OM contents (1.22% to 1.36% and 1.51% to 3.89%, respectively). According to Belayouni [26], this OM makes an absorption/adsorption surface for some metals such as zinc.

Table 3. Whole-rock chemical composition of the input and output products of M'Dhilla-Zone L (ZL) and Redeyef laundries (references of samples are as in Tables 1 and 2).

Elements (%)	Sample							
	RP-ZL	MP-ZL	CW-ZL	FW-ZL	RP-R	MP-R	CW-R	FW-R
OM	1.36	0.60	0.58	1.51	1.22	1.56	1.72	3.89
CaCO ₃	16.87	14.81	27.16	17.47	15.85	14.63	24.19	8.46
N	0.004	0.004	0.003	0.003	0.005	0.005	0.005	0.01
CaO	41.7	47.93	39.6	38.3	45.3	49.51	36.8	21.5
Fe ₂ O ₃	1.44	0.21	1.64	2.34	1.48	0.34	2.25	5.97
Na ₂ O	0.08	0.01	n.a. ¹	0.21	0.02	0.3	n.a.	n.a.
K ₂ O	0.17	0.02	0.16	0.31	0.21	0.04	0.15	0.66
Al ₂ O ₃	1.96	0.51	2.4	3.26	2.13	0.82	2.95	7.34
MgO	1.15	0.46	1.44	1.96	0.89	0.6	1.5	2.25
P ₂ O ₅	25.05	29.37	18.38	18.81	23.28	28.45	15.1	8.45
SiO ₂	10.3	3.84	12.73	14.84	10.03	5.73	20.68	32.29
LOI *	15.1	15.8	22.65	18.8	14.44	13.23	19.47	20.20
CaO/P ₂ O ₅	1.66	1.63	2.15	2.03	1.94	1.74	2.43	2.54
Elements(mg/kg)								
Cd	19.7	17.61	1.34	26	28.8	22	n.d	30.6
Cr	164	122.2	130	302.5	187	147	144.7	466.5
Pb	5.15	1.44	n.d. ²	4.37	3.9	3.4	n.d	8.9
Sr	1307	1583	1096	1240	1392	1507	1007	705
Zn	172	151.6	160	271.6	220	171.5	164	292
U	31	28.87	23	30.2	28.7	35.1	19.35	23
La	48.54	58.8	42.67	49.79	53.98	60.39	29.99	30.25
Ce	77.9	95.3	72.63	78.93	80.72	94.06	42.16	45.49
Nd	49.04	59.33	43.87	50.81	51.24	59.63	23.76	29
Sm	8.69	12.45	8.22	10.47	10.61	12.64	4.98	5.5
Eu	3.15	3.65	2.5	2.64	3.54	3.29	1.93	2.2
Gd	10.3	11.6	9.12	11.33	11.1	13.19	7.65	8.55
Tb	1.63	1.86	1.16	1.39	1.56	1.81	0.83	1.04
Yb	5.14	5.69	4.12	4.96	5.91	6.28	3.12	3.24
∑REE	204.39	248.68	184.3	210.32	218.66	251.29	114.42	125.27

¹ Not analyzed. ² Not detected. * Loss On Ignition

Concerning the total nitrogen, all the samples contain low contents 0.003% to 0.01%; the highest content (0.01%) characterizes the sample FW-R. Likewise, the highest CaCO₃ contents (27.16% to 24.19%) characterize the coarse wastes from the two laundries, thus substantiating the carbonated nature of these wastes.

In terms of major elements, results show that CaO and P₂O₅ have the highest concentrations as major elements for all samples. The highest levels of CaO characterized the marketable phosphate with a maximum of around 49.51% for the Redeyef laundry, and 47.93% for the ZL laundry, whereas the lowest levels are recorded with the fine wastes (Table 3).

Considering the P₂O₅ contents, it is worth noting that the washing process at M'Dhilla-Zone L and Redeyef results in the enrichment of the marketable ore (29.37% and 28.45%, respectively), consequently eliminating the coarse and fine wastes, which are low in phosphate (18.81% and 8.45% P₂O₅, respectively).

With regards to samples extracted from both laundries, the CaO/P₂O₅ ratios show that the values for raw and market phosphates range from 1.63 to 1.94, the lowest values (1.63–1.74) characterize the marketable phosphates. The latter are slightly higher than the corresponding ratio in pure CFA, which is estimated at 1.57 [27]–1.62 [28], indicating that the apatite dealt with is chemically identifiable to CFA [8,29–36]. The higher values obtained for the coarse and fine wastes (2.03–2.54) are indicative of high contents of carbonates as gangue minerals.

The oxides SiO_2 , Al_2O_3 , and Fe_2O_3 characterize mainly the fine wastes (Table 3), which is indicative of the abundance of aluminosilicates in the sludge in both laundries and in particular those of Redeyef (32.29%, 7.34%, and 5.97%, respectively).

Likewise, MgO (1.96% for ZL and 2.25% for Redeyef) is generally known as a component deriving from magnesian clay and dolomite.

Most studies conducted on sedimentary phosphate rocks have shown outstanding enrichment in some trace elements in the apatite [9,26,29,32–34,37–40]. Furthermore, the majority of Cd, Zn, Cr, and U are characterized by their affinity to substitute for Ca in the apatite structure [41].

Strontium content ranged between 705 mg/kg and 1583 mg/kg. The highest levels characterize mainly the marketable and raw phosphates (1583 mg/kg and 1307 mg/kg for M'Dhilla-Zone L, respectively, and 1507 mg/kg and 1392 mg/kg for Redeyef, respectively). High Sr contents (1240 mg/kg) characterize also the fine wastes from M'Dhilla-Zone L (Table 3). Such high Sr contents were reported in the literature [29,30,32–34,38].

Zinc contents ranged between 151.6 mg/kg and 292 mg/kg, with the highest levels detected in fine wastes (271.6 mg/kg for FW-ZL and 292 mg/kg for FW-R), whereas in all other fractions, the contents ranged between 151.6 mg/kg and 220 mg/kg. Although Zn may easily permeate the apatite structure, the high contents observed in the fine wastes, especially in Redeyef, may be attributed to the high content in OM.

The distribution of Cd was different, with the highest concentrations being recorded in both fine wastes (30.6 mg/kg for FW-R and 25.9 mg/kg for FW-ZL) and raw phosphates (19.7 mg/kg for RP-ZL and 28.8 mg/kg for RP-R) (Table 3). With its bivalent state and the ionic radius of 0.97Å [42] being close to that of Ca (0.99Å), Cd can replace Ca in the apatite structure. Therefore, cadmium has been associated with the apatite structure, even though in very small quantities [29,32,34,43]. Equally, cadmium can be also adsorbed by apatite crystals [44].

Chromium content ranged between 122.2 mg/kg and 466.5 mg/kg (Table 3). Fine wastes from the two laundries contained the highest amounts (302.3 mg/kg for FW-ZL and 466.5 mg/kg for FW-R), making up to three times the Cr contents in the other fractions (182 mg/kg to 187 mg/kg). This result shows, firstly, that Cr is essentially associated both to the clay-phosphate fraction and organic matter [29], especially at Redeyef, and secondly, as stipulated by Galfati et al. [8], this result shows that most of this element recorded in fine wastes derives from the corrosion of the process installations (chrome steel-made hydrocyclones).

Uranium distribution shows small fluctuations between the raw phosphates (31 mg/kg for RP-ZL and 28.7 mg/kg for RP-R) and the marketable phosphates (28.87 mg/kg for MP-ZL and 35.1 mg/kg for MP-R). With regards to wastes, U concentrations revealed a small decrease in terms of coarse wastes at M'Dhilla (22.87 mg/kg). Yet, this decrease was noticed with both cases, coarse and fine wastes, at Redeyef (19.35 mg/kg and 23 mg/kg, respectively). These findings indicate that U is evenly distributed between the phosphatic phase and the exogangue at M'Dhilla but is closer to the phosphatic phase at Redeyef.

In terms of raw phosphates, Pb displayed the lowest concentration rate among trace elements (3.9 mg/kg for RP-R and 5.15 mg/kg for RP-ZL). The levels recorded in the output products are slightly variable but more significant in the fine wastes (4.37 mg/kg for FW-ZL and 8.9 mg/kg for FW-R) (Table 3).

In another respect, and compared to other sedimentary rocks, it is generally known that REEs are enriched in marine phosphorites [37,40,41,45–47]. In our samples, and even though characterized by patterns similar in shape, the REEs show variable concentration rates (Table 3), all of which display a slight enrichment in light REEs (LREEs), compared to heavy REEs (HREEs), along with negative Ce and Tb anomalies and a positive Eu anomaly (Figure 3). The cerium anomaly indicates that phosphate has formed in a suboxic to oxic marine environment that is deficient in this element [48]. However, the Tb anomaly, which was previously reported for phosphates in the Gafsa-Métlaoui Basin [8,33,40,49,50], should be relevant in terms of analytical problems only [12,51,52]. According to Fryer [53], the

variations in the Eu contents result from the reduction of this element to the valence 2+, deriving from the modifications observed in the redox conditions. In another respect, the input products (RP) from the two laundries bear almost similar total concentrations (Σ REE of around 204.39 mg/kg for M'Dhilla and 218.66 mg/kg for Redeyef). Similarly, and although the marketable phosphates from both laundries bear more significant total contents in REEs (248.68 mg/kg for MP-ZL and 251.29 mg/kg for MP-R), the coarse and fine wastes still carry considerable quantities of REEs at M'Dhilla-Zone L (184.3 mg/kg and 210.32 mg/kg, respectively) but much lower total contents at Redeyef (114.42 mg/kg and 125.27 mg/kg, respectively). The high contents of REEs in the fine wastes of M'Dhilla are strongly related to their P_2O_5 content (16.87%). As indicated by Slansky [30], it can be stated that REEs have an affinity for phosphates because of their substitution for Ca^{2+} in the apatite structure, on the one hand, and their correlation with the organic matter present in pellets, on the other.

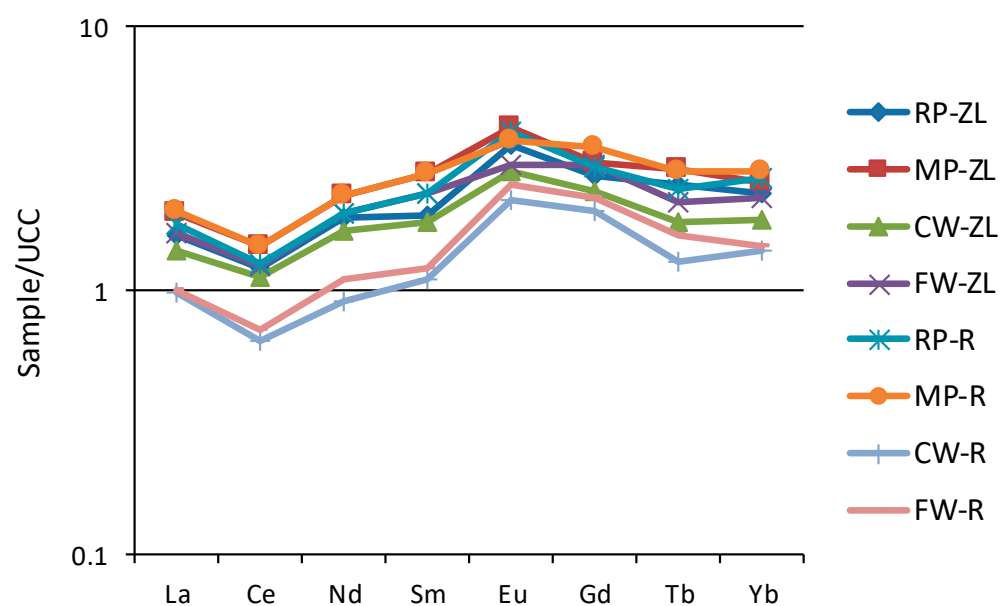


Figure 3. The rare-earth element (REE) patterns normalized to the upper continental crust (UCC) of raw phosphate (RP), marketable phosphate (MP), fine waste (FW), and coarse waste (CW) from M'Dhilla-Zone L (ZL) and Redeyef (R).

3.1.4. Water Quality

The water samples collected from drilling water (DW), recycled water (RW), and sludge water (SW) and recovered from the laundries after natural decantation and filtration, were submitted to chemical analysis in order to determine the anion (F^- , NO_2^- , NO_3^- , PO_4^{3-} , and SO_4^{2-}) and trace element (Cd, Fe, Pb, Zn, and U) contents. Table 4 presents the results.

The pH values of the discharge water, which were measured in situ, at the exit of the laundries were 7.87 at M'Dhilla-ZL and 7.07 at Redeyef, reflecting the slight alkaline nature of the wastewater. The feedwater used in the phosphate washing units comes from the various aquifers in the region. At M'Dhilla, the wash (drilling) water shows high loads, exceeding the World Health Organization (WHO) standards, in sulfates (1979 mg/L), fluorine (23.75 mg/L), and nitrites (15.3 mg/L), while the sludge water is heavily loaded with sulfates (2570 mg/L), fluorine (47 mg/L), and cadmium (14.14 μ g/L). At Redeyef, the wash water is rich in fluorine (1.9 mg/L), while the sludge water is contaminated with Cd (6.12 μ g/L).

Table 4. Results of chemical analysis of drilling water (DW), sludge water (SW), and recycled water (RW) from M'Dhillia-Zone L (ZL) and Redeyef (R) laundries.

Element (mg/L)	Laundry ZL			Laundry R			Regulation Limit ¹
	Gouifla (DW)	Sludge Water (SW)	Recycled Water (RW)	Tarfaya (DW)	Sludge Water (SW)	Recycled Water (RW)	
F ⁻	2.37	4.7	2.32	1.9	0.77	1.28	1.5
NO ₂ ⁻	15.30	<d.l. ³	1.57	0.34	0.32	<d.l.	3
NO ₃ ⁻	17.70	48.6	17.15	32.74	32.88	32.94	50
PO ₄ ³⁻	14	24.8	15.40	22.2	33	23.6	- ⁴
SO ₄ ²⁻	1979	2570	2495	51.2	312.5	22.7	500
Element (µg/L)							
Cd	1	14.14	5	1	6.12	1	3
Fe	10	10	10	10	10	10	-
Pb	2	1	2	4	2	3	10
Zn	19	53	21	20	66	14	3000
U	n.a. ²	1.58	n.a	n.a	3.13	n.a	15

¹ WHO standards for potable water, updated in 2006. ² Not analyzed. ³ Below the detection limit. ⁴ No guide value.

3.2. Evaluation of Fine Waste-Iron Mobility: Batch Experiments

In this study, batch tests were carried out to assess the potential mobility and hydro solubility of MTE contained in the fine wastes of the laundries of the study area.

3.2.1. pH and Conductivity

The pH variations of the leachate representative of the whole cycles of the test are provided in Figure 4. The pH values recorded for the leachate of the sample FW-ZL show a gradual increase from a minimum of 7.07 to a maximum of 7.73 during the second cycle, followed by a decrease until stabilization during the last three cycles at a value close to 7.55. The increased portion in pH could be explained by the dissolution of CaCO₃, the content of which is higher in these wastes (Table 3). However, pH values of the sample FW-R gradually decrease from 7.87, before they stabilize again during the last three cycles at 7.45.

Results of the EC measured on the leachates in both samples FW-ZL and FW-R are displayed by the two curves provided in Figure 4. This phenomenon shows an increase during the first cycle, then the conductivity decreases during the second cycle, and stabilizes during the subsequent cycles. It is shown, however, that the EC values are high for both samples, but those measured for FW-ZL (10.97 ms/cm to 20 ms/cm) are much larger compared to those of FW-R (3.85 ms/cm to 7.85 ms/cm), indicating a greater ionic charge in the solution for FW-ZL.

The high values of EC can be explained by the dissolution of the more soluble minerals, such as gypsum and calcite (Table 2). The highest values characterizing the first cycle for the leachates of both samples can be explained by the solubilization of the gypsum contained in the fine wastes [54]. Subsequently, the stable conductivity values during the last four cycles may be attributed to the stability of the leached ion fluxes.

3.2.2. Mobilisation of Cd and U

The concentrations of Cd and U, as measured in the leachate from batch tests, are displayed in Figure 5. First, we shall underscore the similarity in the behavior of the two elements throughout the seven cycles for both waste samples; both show a general tendency to increase during the first four cycles to a maximum (17.53 µg/L and 4.41 µg/L, respectively, for M'Dhillia, and 8.68 µg/L and 3.78 µg/L, respectively, for Redeyef), and with a stabilization (plateau) over the last three cycles, indicating the stability of the fluxes of both elements that go into solution during each cycle at this stage of the experiment. These results show that cadmium is more mobile than uranium because its mobility is more pronounced for the sample FW-ZL. However, the cadmium contents in the leachate, recovered during both batch experiments (11.9 µg/L–17 µg/L for FW-ZL and 5.4 µg/L–8.7 µg/L for FW-R), exceed the WHO standards required for potable water (3 µg/L).

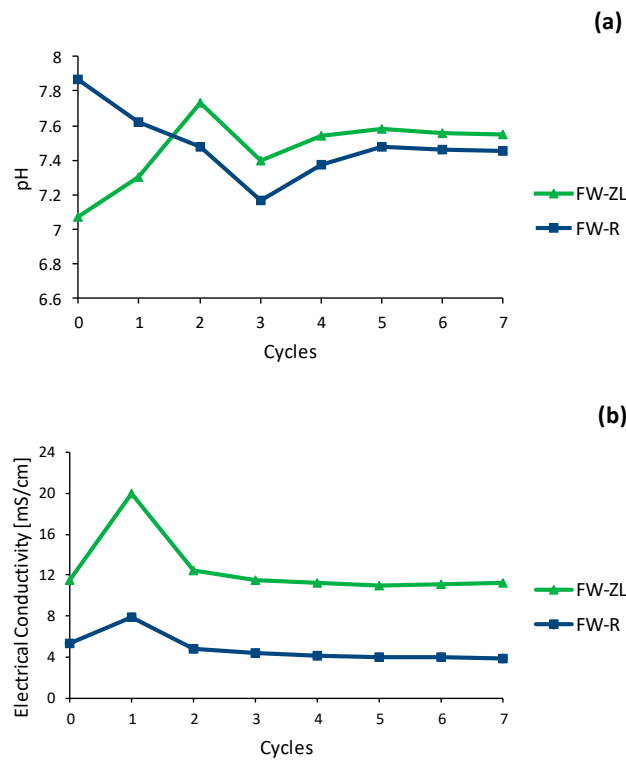


Figure 4. Variation of (a) pH and (b) electrical conductivity (mS/cm) of the leachates during the seven cycles of the batch test (FW-R: fine waste in the sludge from Redeyef and FW-ZL: fine waste in the sludge from M’Dhilla-Zone L).

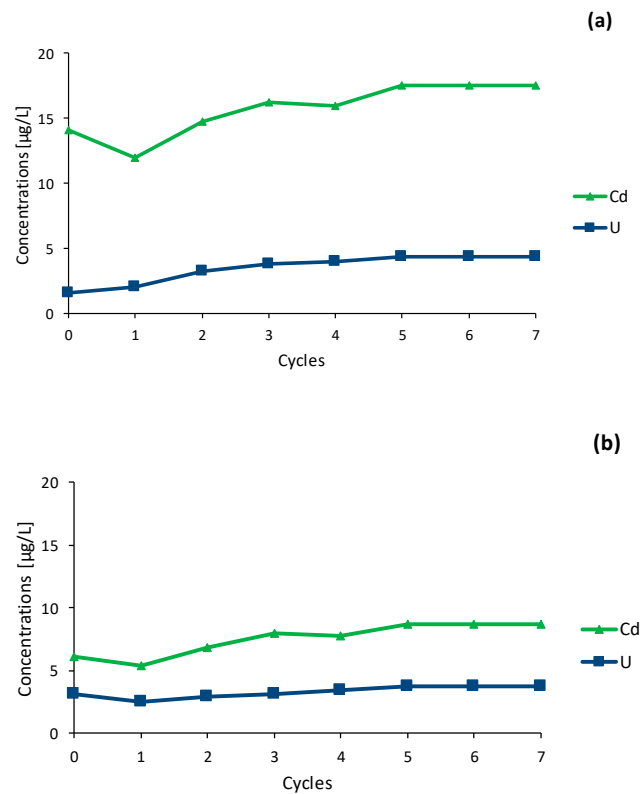


Figure 5. Concentrations of Cd and U in the leachates of the seven batch cycles. (a) FW-ZL: fine waste from M’Dhilla-Zone L laundry and (b) FW-R: fine waste from Redeyef laundry.

The percentages of Cd and U mobility in the solid fraction of the sludge, which are calculated from the ratio between the concentrations mobilized by the extractant (sludge water) to the total concentration of MTE, show that the mobility of both elements is low, with percentages not exceeding 0.067% and 0.014%, respectively, for M'Dhilla, and 0.028% and 0.016% for Redeyef.

3.3. Discussion

The fine petrographic, mineralogical, and geochemical characterization showed significant differences between the two sludge samples analyzed.

Equally, the particle-size distribution showed that the sludge from the Redeyef laundry is enriched in fine fraction (82.84%) compared to that from M'Dhilla-ZL (58.87%).

The mineralogical study showed the presence of the following minerals in the two fine wastes: CFA, clinoptilolite, calcite, dolomite, gypsum, ankerite, quartz, and other silicates, such as smectite and palygorskite. We also deduced that the latter are more abundant in the fine wastes of the Redeyef laundry.

The wet processing of raw phosphate is a simple physical process of granulometric classification resulting in the separation of the merchant ore (71 μm –2000 μm) enriched in CFA, from the fine (–71 μm) and coarse (+2000 μm) fractions enriched in gangue minerals (carbonates, silicates, etc.).

Chemical analysis showed that carbonates, P_2O_5 , U, and REEs are more abundant in the fine wastes from M'Dhilla-ZL (17.47%, 18.81%, 30.2 mg/kg, and 210.3 mg/kg, respectively), whereas higher contents in organic matter, Fe_2O_3 , and Al_2O_3 characterize the sludge from Redeyef (3.89%, 5.97%, and 7.34%, respectively). It should be noted, however, that Cd, Cr, and Zn are more concentrated in the fine wastes of both laundries, as compared to their content in the raw phosphate.

Batch experiments showed that, although the two fine waste samples of M'Dhilla-ZL and Redeyef laundries contain close total contents in Cd (26 mg/kg and 30.6 mg/kg, respectively); and U (30.2 mg/kg and 23 mg/kg, respectively), they behaved quite differently during the tests.

With regards to pH conditions, the slightly alkaline conditions prevailed during the whole test. As a result, heavy metals are characterized by low mobility due to precipitation reactions, and the increase of adsorption sites is linked to OM (carboxyl groups), oxyhydroxides, and clay minerals [55,56], as well as the decrease of H^+ ions competition for adsorption [57]. Furthermore, the higher content in clay–phosphate fraction, clinoptilolite, and OM in the fine wastes of Redeyef (FW–R) seemed to have played a role in the retention of Cd, consequently, its low mobility with respect to Cd in the case of the equivalent sample from M'Dhilla-ZL (FW–ZL).

Considering the sample FW–R, Cd could be associated with the phosphatic phase and adsorbed on the surface of silicate minerals (clays and clinoptilolite), which are plentiful in fine fractions. Besides aluminosilicates, these fine wastes contain also high amounts of OM (Table 3). Both of them are capable of adsorbing cadmium, consequently reducing its mobility [58], which makes it difficult to be released by leaching. Indeed, thanks to their very large specific surfaces (up to 800 m^2/g) and their great cation-exchange capacities, organic matter and silicate minerals are believed to be excellent absorbents [59–61]. Clinoptilolite, with its cavernous structure, has a very high selective retention capacity for certain heavy metals, in particular Cd [62].

With regards to the sample FW–ZL, the significant mobility of Cd is attributed to its high content of phosphate and low content of silicate minerals, with high metal adsorption capacity. In freshwater, aqueous species of cadmium consist of Cd^{2+} , $\text{Cd}(\text{OH})_2^0$, and CdHCO_3^- [63], among which Cd^{2+} is the dominant ionic species up to pH 8 [64–67], which is a free and very reactive (bioavailable) form [58,68–70].

Likewise, the adsorption phenomenon by aluminosilicates and the carbonated nature of the two fine wastes may account for the small quantities of released uranium. As postulated by Altschuler et al. [71], Sassi [29], Baturin et al. [72], Giresse et al. [73], and

Chaabani [32], an important part of uranium is adsorbed onto apatite in an oxidized form. According to Sassi [29] and Favas et al. [74], uranium can also be adsorbed on clays and other organic matter.

In natural water, uranium can exist mainly as U^{4+} and U^{6+} ions, the abundance of which is influenced by the presence and the profusion of complexing agents, as well as the prevailing pH and Eh conditions [75–78]. U (IV) is the most dominant form in reducing environments, while U (VI) is prevalent in oxidizing environments [79,80]. Furthermore, tetravalent U is extremely resistant to leaching, whereas hexavalent U is highly mobile. At pH > 5, U mobility is due to the complexation of uranyl ions (UO_2^{2+}) by carbonate, phosphate, and hydroxyl species [74–76,78,80–84]. Besides pH and Eh, uranyl speciation may also be influenced by organic ligand concentration [81], as long as the two fine wastes being considered bear high amounts of organic matter (Table 3).

4. Conclusions

This study, dealing with the input and output products of the laundries of Redeyef and M'Dhilla-ZL in the Gafsa-Metlaoui Basin, has shown that these products bear the same mineral assemblages (CFA, calcite, dolomite, ankerite, quartz, gypsum, and clinoptilolite), with varying proportions from fraction to fraction. Also, geochemical analyses have revealed that the majority of metallic elements (Cr, Zn, Cd, and Pb) are most often concentrated in the fine wastes (<71 μ m) and associated with the clay–phosphate fraction, whereas the contents of rare earth elements and U are higher in the marketable and raw phosphate fractions.

The geochemical study of the water shows that, at M'Dhilla, the feed (drilling) water, which is used for washing, is loaded with sulfates (1979 mg/L), fluorine (2.37 mg/L), and nitrites (15.3 mg/L), while the sludge water is loaded with even more sulfates (2570 mg/L) and fluorine (4.7 mg/L), besides Cd (14.14 μ g/L). At Redeyef, the feedwater is slightly loaded with fluorine (1.9 mg/L), while the sludge water is loaded with Cd (6.12 μ g/L). Equally, the leaching tests that were conducted on fine wastes from both laundries have revealed that only small proportions of Cd and U are mobilized ($\leq 0.07\%$ and $\leq 0.02\%$, respectively).

These results show that, in both localities, feed (drilling) and process (sludge) water, which are loaded with fluorine and cadmium, along with sulfate at M'Dhilla, exceed the WHO standards for potable water for fluoride (M'Dhilla and Redeyef), cadmium (M'Dhilla and Redeyef), and sulfate (M'Dhilla), indicating that these elements account for the water resource pollution in the region. This pollution rate is even more conspicuous in M'Dhilla than in Redeyef.

These results should prompt the CPG to review its strategy for managing discharges from the phosphate industry, especially to safeguard both surface and underground water resources in the region.

Author Contributions: Contributed to the study conception and design: F.S. and O.S.; Methodology: O.S. and M.S.; Investigation: O.S. and M.S.; Resources: R.S., O.S., and M.S.; Writing—Original draft preparation: O.S. and M.S.; Writing—Review and Editing: F.S. and R.S.; Supervision: F.S. and R.S.; Project administration: F.S. All authors have read and agreed to the published version of the manuscript.

Funding: This research received no external funding.

Acknowledgments: The authors would like to thank Faysal Souissi, English Department, Faculty of Humanities of Tunis, University of Tunis, for his kind and thorough review and proof-reading of the English version of this manuscript. Thanks go also to the Compagnie des Phosphates de Gafsa (CPG) for all the facilities granted during the sampling campaigns carried out in the laundries.

Conflicts of Interest: The authors declare no conflict of interest.

References

1. U.S. Geological Survey (USGS). *Mineral Commodity Summaries 2020*; U.S. Government Publishing Office: Reston, VA, USA, 2020.
2. Ruan, Y.; He, D.; Chi, R. Review on beneficiation techniques and reagents used for phosphate ores. *Minerals* **2019**, *9*, 253. [CrossRef]
3. Boujljel, H.; Daldoul, G.H.; Tlil, H.; Souissi, R.; Chebbi, N.; Fattah, N.; Souissi, F. The beneficiation processes of low-grade sedimentary phosphates of Tozeur-Nefta deposit (Gafsa-Métlaoui Basin: South of Tunisia). *Minerals* **2019**, *9*, 2. [CrossRef]
4. Groupe-conseil Genivar Inc (GCGI); Société Centrale pour l'Équipement du Territoire (SCET). *Environmental Impact Study of the Fine Discharges from the Phosphate Laundries of the Compagnie des Phosphates de Gafsa. Phase I, Step A: Description of the Receiving Environment*; Internal Report; The Compagnie des phosphates de Gafsa, Document SCET: Tunis, Tunisia, 2001.
5. Mhemdi, S. *Study of Fine Discharges from Laundries and the Phosphate Processing Industry and Their Impact on the Environment*; D.A.S., University of Tunis II: Tunis, Tunisia, 1999.
6. Ounis, A. Environmental characterization of the M'Dhillia region (South Gafsa Basin). In *Study of Discharges from the M'Dhillia Plant and the Gafsa Phosphate Company's Laundries*; D.A.S., University of Tunis El Manar: Tunis, Tunisia, 2002.
7. Galfati, I.; Bilal, E.; Beji Sassi, A.; Abdallah, H.; Zaeir, A. Accumulation of heavy metals in native plants growing near the phosphate treatment industry, Tunisia. *Carpathian J. Earth Environ. Sci.* **2011**, *6*, 85–100.
8. Galfati, I.; Bilal, E.; Abdallah, H.; Sassi, A.B. Geochemistry of solid effluents and phosphate ore washed from Métlaoui-Gafsa Basin, Tunisia. *Rom. J. Mineral. Depos.* **2014**, *87*, 83–86.
9. Chokri, A.; Hatira, A.; Zarai, N.; Abdeljaouad, S. Impact of discharges from phosphate laundries on the concentration of heavy metals in soils and plants in the Gafsa-Métlaoui mining basin (Southwest Tunisia). *Rev. Méditerranéenne L'Environnement* **2006**, *1*, 121–134.
10. Galfati, I. Study of the phosphorites of Jbel Oum EL Khecheb and Impact of Discharges from the Phosphate Industry on the Environment in the Gafsa-Métlaoui Basin. Ph.D. Thesis, University of Tunis El Manar, Tunis, Tunisia, 2010.
11. Giroux, M.; Audesse, P. Comparison of two methods for the determination of organic carbon, total nitrogen and C/N ratio of various organic amendments and farmyard fertilizers. *Agrosol Revue Agroenvironnement* **2004**, *15*, 107–110.
12. Taylor, S.R.; McLennan, S.M. *The Continental Crust: Its Composition and Evolution*; Blackwell Scientific Publications: Oxford, UK, 1985.
13. Juste, C. Application of mobility and bioavailability of trace elements in soil. *Sci. Du Sol.* **1988**, *26*, 103–112.
14. Manceau, A.; Marcus, M.A.; Tamura, N. Quantitative speciation of heavy metals in soils and sediments by synchrotron X-ray techniques. In *Reviews in Mineralogy and Geochemistry Applications of Synchrotron Radiation in Low-Temperature Geochemistry and Environmental Science*; Fenter, P., Rivers, M., Sturchio, N.C., Sutton, S., Eds.; Mineralogical Society of America: Washington, DC, USA, 2002; pp. 341–428.
15. Sigg, L.; Behra, P.; Stumm, W. *Chemistry of aquatic environments—Chemistry of natural waters and interfaces in the environment*; Dunod: Paris, France, 2000.
16. Deurer, R.; Forstner, U.; Schmoll, G. Selective chemical extraction of carbonate-associated metals from recent lacustrine sediments. *Geochim. Cosmochim. Acta* **1978**, *42*, 425–427. [CrossRef]
17. Gibbs, R.J. Mechanism of trace metal transport in rivers. *Nature* **1973**, *180*, 71–73. [CrossRef]
18. Cameron, E.M. Geochemical methods of exploration for massive sulphide mineralization in the Canadian Shield. In *Geochemical Exploration*; Elliott, I.L., Fletcher, W.K., Eds.; Elsevier: Amsterdam, The Netherlands, 1974; pp. 21–49.
19. Kim, A.G. Leaching methods applied to the characterization of coal utilization by-products. Proceedings of Regulation Risk, and Reclamation with Coal Combustion by-Products at Mines; Vories, K.C., Harrington, A., Eds.; A technical inetractive forum, Held in Conjunction with the World of Coal Ash. Lexington Center, Heritage Hall: Lexington, KY, USA, 2005; pp. 89–96.
20. Esakku, S.; Karthikeyan, O.P.; Joseph, K.; Nagendran, R. Heavy Metal Fractionation and Leachability Studies on Fresh and Partially Decomposed Municipal Solid Waste. *Pract. Period. Hazard. Toxic Radioact. Waste Manag.* **2008**, *12*, 127–132. [CrossRef]
21. Kosson, D.S.; Van der Sloot, H.A.; Sanchez, F.; Garrabrants, A.C. An Integrated Framework for Evaluating Leaching in Waste Management and Utilization of Secondary Materials. *Environ. Eng. Sci.* **2002**, *19*, 159–204. [CrossRef]
22. Townsend, T.; Jang, Y.C.; Tolaymat, T. A Guide to the Use of Leaching Tests in Solid Waste Management Decision Making, Report #03-01(A), Prepared for: The Florida Center for Solid and Hazardous Waste Management, University of Florida. 2003. Available online: <https://semspub.epa.gov/work/09/1112378.pdf> (accessed on 3 September 2020).
23. Van Der Sloot, H.A.; Heasman, L.; Quevauvillier, P. *Harmonization of Leaching/Extraction Tests*; Elsevier Science: Amsterdam, The Netherlands, 1997; eBook; ISBN 9780080533308.
24. Lassin, A.; Bodénan, F.; Piantone, P.; Blanc, P. *Tests of Waste Behaviour during Leaching and Modelling of the Associated "Hydro-Physico-Chemical" Processes*; Bibliographical Study, BRGM/RP-51518-FR.; B.R.G.M: Orleans, France, 2002.
25. Garrabrants, A.C.; Kosson, D.S.; Van der Sloot, H.A.; Sanchez, F.; Hjelmar, O. *Background Information for the Leaching Environmental Assessment Framework (LEAF) Test Methods*; U.S. Environmental Protection Agency: Washington, DC, USA, 2010; EPA-600/R-10/170.
26. Belayouni, H. Study of the Organic Matter in the Phosphate Series of the Gafsa-Métlaoui Basin (Tunisia). Ph.D. Thesis, University of Orléans, Orléans, France, 1983.
27. McLennan, G.H.; Lehr, J.R. Crystal chemical investigation of natural apatites. *Am. Mineral.* **1969**, *54*, 1374–1391.

28. Gadd, M.G.; Layton-Matthews, D.; Peter, J.M. Non-hydrothermal origin of apatite in SEDEX mineralization and host rocks of the Howard's Pass district, Yukon, Canada. *Am. Mineral.* **2016**, *101*, 1061–1071. [[CrossRef](#)]
29. Sassi, S. Phosphate Sedimentation in the Paleocene in Southern and Central Tunisia. Ph.D. Thesis, University of Paris–Sud, Orsay, France, 1974.
30. Slansky, M. *Geology of Sedimentary Phosphates*; B.R.G.M: Orleans, France, 1980.
31. McLennan, G.H.; Van Kauwerberch, S.V. Clay mineralogy of the phosphorites of the southeastern United States. In *Phosphate Deposits from the World: Genesis of Neogene to Recent Phosphorite*; Riggs, S.R., Burnet, W.L., Eds.; Cambridge University Press: Cambridge, UK, 1990; pp. 337–351.
32. Chaabani, F. Dynamics of the Eastern Part of the Gafsa Basin in the Cretaceous and Paleogene. Mineralogical and Geochemical Study of the Eocene—Southern Tunisia Phosphate Series. Ph.D. Thesis, University of Tunis El Manar, Tunis, Tunisia, 1995.
33. Beji-Sassi, A. Phosphates in the Paleogenic Basins of the Southern Part of the North-South Axis. Ph.D. Thesis, University of Tunis El Manar, Tunis, Tunisia, 1999.
34. Zaier, A. Tectono-Sedimentary Evolution of the Phosphate Basin of Central Western Tunisia: Mineralogy, Petrography, Geochemistry and Genesis of Phosphorites. Ph.D. Thesis, University of Tunis El Manar, Tunis, Tunisia, 1999.
35. Boughzala, K.H.; Fattah, N.; Bouzouita, K.H.; Ben Hassine, H. Mineralogical and chemical study of Oum El Khecheb rock phosphate (Gafsa, Tunisia). *Rev. Sci. Des Matériaux Lab. LARHYSS* **2015**, *6*, 11–29.
36. Gallala, W.; Saïdia, M.; El Hajjib, S.; Zayani, K.; Gaied, M.E.; Montacer, M. Characterization and Valorization of Tozeur-Nefta Phosphate Ore Deposit (Southwestern Tunisia). *Procedia Eng.* **2016**, *138*, 8–18. [[CrossRef](#)]
37. Altschuler, Z.S. The geochemistry of trace elements in marine phosphorites: Part I. characteristic abundances and enrichment. *Soc. Econ. Paleontol. Mineral.* **1980**, *29*, 19–30.
38. Chaabani, F. Phosphorites of the Fom Selja Type Section (Metlaoui, Tunisia): A Sequential Sedimentary Series with Paleocene Evaporites. Ph.D. Thesis, University of Louis Pasteur, Strasbourg, France, 1978.
39. Beji-Sassi, A. Petrology, Mineralogy and Geochemistry of Phosphate Sediments of the Eastern Border of the Island of Kasserine (Tunisia). Ph.D. Thesis, University of Tunis El Manar, Tunis, Tunisia, 1984.
40. Garnit, H.; Bouhleb, S.; Jarvis, I. Geochemistry and depositional environments of Paleocene-Eocene phosphorites: Mélaoui Group, Tunisia. *J. Afr. Earth Sci.* **2017**, *134*. [[CrossRef](#)]
41. Jarvis, I.; Burnett, W.C.; Nathan, Y.; Almbaydin, F.; Attia, K.M.; Castro, L.N.; Flicoteaux, R.; Hilmy, M.E.; Husain, V.; Qutawna, A.A.; et al. Phosphorite geochemistry: State-of-the-art and environmental concerns. *Eclogae Geol. Helv.* **1994**, *87*, 643–700.
42. Cordero, B.; Gómez, V.; Platero-Prats, A.E.; Revés, M.; Echeverría, J.; Cremades, E.; Flavia Barragán, F.; Santiago Alvarez, S. Covalent radii revisited. *Dalton Trans.* **2008**, *21*, 2832–2838. [[CrossRef](#)]
43. Beji-Sassi, A.; Sassi, S. Cadmium associated with phosphate deposits in southern Tunisia. *J. Afr. Earth Sci.* **1999**, *29*, 501–513.
44. Ahrens, L.H. *Origin and Distribution of the Elements*; Pergamon Press: Paris, France, 1977.
45. Semenov, E.I.; Kholodov, V.N.; Barinsky, R.L. Rare earths in phosphorites. *Geokhimiya* **1962**, *5*, 434–439.
46. Dill, H.G.; Weiss, W.; Botz, R.; Dohrmann, R. Paleontological, mineralogical and chemical studies of syngenetic and epigenetic Pb–Zn–Ba–P mineralizations at the stratotype of the K/P boundary (El Kef area, Tunisia). *Int. J. Earth Sci.* **2010**, *100*, 805–846. [[CrossRef](#)]
47. Garnit, H.; Bouhleb, S.; Barca, D.; Johnson, C.A.; Chtara, C. Phosphorite-hosted zinc and lead mineralization in the Sekarna deposit (Central Tunisia). *Miner. Depos.* **2011**, *47*, 545–562. [[CrossRef](#)]
48. Pattan, J.N.; Pearce, N.J.G.; Mislankar, P.G. Constraints in using Cerium-anomaly of bulk sediments as an indicator of paleobottom water redox environment: A case study from the Central Indian Ocean Basin. *Chem. Geol.* **2005**, *221*, 260–278. [[CrossRef](#)]
49. Tlig, S.; Beji Sassi, A.; Belayouni, H.; Michel, D. Distribution of Uranium, Thorium, Zirconium, Hafnium and Rare Earth Elements (REE) in sedimentary phosphate grains. *Chem. Geol.* **1987**, *62*, 209–221. [[CrossRef](#)]
50. Ounis, A.; Kocsis, L.; Chaabani, F.; Rudolf Pfeifer, H. Rare earth elements and stable isotope geochemistry ($\delta^{13}\text{C}$ and $\delta^{18}\text{O}$) of phosphorite deposits in the Gafsa Basin, Tunisia. *Palaeogeogr. Palaeoclimatol. Palaeoecol.* **2008**, *268*, 1–18. [[CrossRef](#)]
51. Elderfield, H.; Greaves, M.J. The rare earth elements in seawater. *Nature* **1982**, *296*, 214–219. [[CrossRef](#)]
52. McLennan, S.M. REE in sedimentary rocks: Influence of provenance and sedimentary processes. *Rev. Mineral.* **1989**, *21*, 169–200.
53. Fryer, B. Rare earth evidence in iron-formations for changing Precambrian oxidation states. *Geochim. Cosmochim. Acta* **1977**, *41*, 361–367. [[CrossRef](#)]
54. Souissi, R.; Souissi, F.; Chakroun, H.K.; Bouchardon, J.L. Mineralogical and geochemical characterization of the mine tailings and assessment of Zn, Cd, Pb mobility in a carbonated setting (northern Tunisia). *Mine Water Environ.* **2013**, *32*, 16–27. [[CrossRef](#)]
55. Godfrin, J.M.; Bladel, R.V. Influence of pH on the adsorption of copper and zinc by soils. *Sci. Du Sol.* **1990**, *28*, 15–26.
56. Gould, M.S.; Genetelli, E.J. Heavy metal complexation behavior in anaerobically digested sludges. *Water Res.* **1978**, *12*, 505–512. [[CrossRef](#)]
57. Pigozzo, A.T.J.; Lenzi, E.; Junior, J.L.; Scapim, C.A.; Da Costa, A.C.S. Transition Metal Rates in Latosol Twice Treated With Sewage Sludge. Brazil. *Arch. Biol. Technol.* **2006**, *49*, 515–526. [[CrossRef](#)]
58. Institut de Radioprotection et de Sûreté Nucléaire (IRSN). Radionuclide Sheet: Cadmium and Environment. 2004. Available online: https://www.irsn.fr/FR/Larecherche/publications-documentation/fiches-radionucleides/Documents/environnement/Cadmium_Cd109_v1.pdf (accessed on 10 January 2020).

59. Tollefson, T. Soils and Their Environment. Department of Soil Science University of Saskatchewan. Text Translated by Bélanger N. 2005. Available online: http://www.cef-cfr.ca/uploads/Membres/module_4_sols.pdf (accessed on 15 December 2018).
60. Mermoud, A. Basic Properties of the Soil and the Liquid Phase. Soil Physics Course. 2006. Available online: <https://fr.scribd.com/document/338544201/02-Proprietes-de-base-du-sol-et-de-la-phase-liquide-pdf> (accessed on 12 January 2018).
61. Deschamps, T.; Benzaazoua, M.; Bussiere, B.; Belem, T.; Mbonimpa, M. Retention mechanisms for heavy metals in the solid phase: The case of the stabilization of contaminated soils and industrial waste. *Rev. Electron. Sci. L'environnement* **2006**. [CrossRef]
62. Babel, S.; Kurniawan, T.A. Low-cost adsorbent for heavy metal uptake from contaminated water: A review. *J. Hazard. Mater.* **2003**, *97*, 219–243. [CrossRef]
63. Rose, A.W.; Hawks, H.E.; Webb, J.H. *Geochemistry in Mineral Exploration*. Academic Press: New York, NY, USA, 1979.
64. Cossa, D.; Lassus, P. *Cadmium in the Marine Environment/Biogeochemistry and Ecotoxicology*; IFREMER Scientific and Technical Report N°16; Ifremer: Plouzané, France, 1989.
65. National Research Council (NRC). *Subcommittee on Zinc Cadmium Sulfide, Toxicologic Assessment of the Army's Zinc Cadmium Sulfide Dispersion Tests*; National Academies Press (US): Washington, DC, USA, 1997.
66. Marchat, D. Fixation of Cadmium by a Phosphocalcic Hydroxyapatite—Kinetic and Thermodynamic Study. Ph.D. Thesis, University of Limoges, Limoges, France, 2005.
67. Health Canada. Cadmium in Drinking Water. Guideline Technical Document for Public Consultation. 2019. Available online: <https://www.canada.ca/en/health-canada/programs/consultation-cadmium-drinking-water/document.html> (accessed on 15 April 2019).
68. Health Canada. Priority Substances List, Assessment Report, Cadmium and Its Compounds. Canadian Environmental Protection Act. 1994. Available online: https://www.canada.ca/content/dam/hc-sc/migration/hc-sc/ewh-semt/alt_formats/hecs-sesc/pdf/pubs/contaminants/psl1-lsp1/cadmium_comp/cadmium_comp-fra.pdf (accessed on 12 April 2019).
69. Gauthier, J. *Cadmium Toxicity and Bioaccumulation in Juvenile Atlantic Salmon (Sa/mo sa/ar) in the Presence of Synthetic or Natural Dissolved Organic Matter (DOM)*; Institut National de la Recherche Scientifique, INRS-Eau Sainte-Foy: Québec, QC, Canada, 1995.
70. Qasim, B.H. Determination, Speciation and Bioavailability of Metallic Trace Elements in Contaminated Soils and Techno Soils. Ph.D. Thesis, University of Orléans, Orléans, France, 2015.
71. Altschuler, Z.S.; Clarke, R.S.; Young, E.J. Geochemistry of uranium in apatite and phosphorites. *US Geol. Surv.* **1958**, *314*, 87.
72. Baturin, G.N.; Dubinchuk, V.T. Microstructures of Agulhas Banks phosphorites. *Mar. Geol.* **1974**, *16*, M63–M70. [CrossRef]
73. Giresse, P.; N'landou, J.D.; Wiber, M. Uranium concentrations of phosphates in the Congo according to marine and continental mineralogensis. *Bull. Geol. Fr.* **1984**, *7*, 1097–1105. [CrossRef]
74. Favas, P.J.C.; Pratas, J.; Mitra, S.; Sarkar, S.K.; Venkatachalam, P. Biogeochemistry of uranium in the soil-plant and water-plant systems in an old uranium mine. *Sci. Total Environ.* **2016**, *568*, 350–368. [CrossRef]
75. Langmuir, D. *Aqueous Environmental Geochemistry*; Prentice Hall: Englewood Cliffs, NJ, USA, 1997.
76. Lottermoser, B.G. *Mine Wastes Characterization, Treatment, Environmental Impacts*; Springer: Berlin/Heidelberg, Germany, 2007.
77. Laurette, J.; Larue, C.; Mariet, C.; Brisset, F.; Khodja, H.; Bourguignon, J.; Marie Carriere, M. Influence of uranium speciation on its accumulation and translocation in three plant species: Oilseed rape, sunflower and wheat. *Environ. Exp. Bot.* **2012**, *77*, 96–107. [CrossRef]
78. Qiao, J.; Hansen, V.; Hou, X.; Aldahan, A.; Possnert, G. Speciation analysis of ¹²⁹I, ¹³⁷Cs, ²³²Th, ²³⁸U, ²³⁹Pu and ²⁴⁰Pu in environmental soil and sediment. *Appl. Radiat. Isot.* **2012**, *70*, 1698–1708. [CrossRef] [PubMed]
79. United States Environmental Protection Agency (EPA). Understanding Variation in Partition Coefficient, K_d, Values: Volume I, The K_d Model, Methods of Measurement, and Application of Chemical Reaction Codes (EPA402-R-99-004A). 1999. Available online: <https://www.epa.gov/sites/production/files/2015-05/documents/402-r-99-004a.pdf> (accessed on 15 May 2019).
80. Commissariat à L'énergie Atomique (CEA). Uranium in the Environment. 2001. Available online: https://inis.iaea.org/collection/NCLCollectionStore/_Public/33/003/33003392.pdf (accessed on 10 April 2019).
81. Institut de Radioprotection et de Sureté Nucléaire (IRSN). Radionuclide File: Natural Uranium and the Environment. 2010. Available online: <https://www.irsn.fr/FR/Larecherche/publications-documentation/fiches-radionucleides/environnement/Pages/Uranium-naturel-environnement.aspx#.XmedwnL7TIU> (accessed on 10 May 2018).
82. Laurette, J. Role of Speciation of Uranium on Its Bioaccumulation, Transport, and Toxicity in Plants. Ph.D. Thesis, University of ParisTech, Paris, France, 2011.
83. Pratas, J.; Favas, P.J.C.; Paulo, C.; Rodrigues, N.; Prasad, M.N.V. Uranium accumulation by aquatic plants from uranium-contaminated water plants in Central Portugal. *Int. J. Phytoremediation* **2012**, *14*, 221–234. [CrossRef] [PubMed]
84. Harguindégui, S. Uranium Transport in Water and Soil: Combined Colloidal and Isotopic Approach. Ph.D. Thesis, University of Pau and the Adour Region, Pau, France, 2013.